

## Spin physics with STAR at RHIC

C.A. Gagliardi, T. Lin, R.E. Tribble, and the STAR Collaboration

Our group continues to play major roles in STAR investigations of both longitudinal and transverse spin phenomena in polarized  $pp$  collisions at RHIC. A major goal of the RHIC spin program is to determine the gluon polarization in the proton over a wide range of momentum fraction  $x$ . The longitudinal double-spin asymmetries,  $A_{LL}$ , for inclusive jet and di-jet production are ideal tools in this effort because the cross sections are large and dominated by quark-gluon and gluon-gluon scattering processes, both of which have large partonic asymmetries.

As discussed in previous *Progress in Research* issues, our former graduate student, Zilong Chang, performed an analysis of  $A_{LL}$  for inclusive jet production in 510 GeV  $pp$  collisions, using data that STAR collected during 2012. The results will provide new constraints on the gluon polarization in the region  $0.015 < x < 0.2$ , including the region  $x < 0.05$  that isn't sampled by mid-rapidity jet production in 200 GeV collisions. A decision was made to combine the 2012 inclusive jet  $A_{LL}$  results with the di-jet  $A_{LL}$  measurements that are based on the same data set and were analyzed at University of Kentucky. As of this writing, the paper draft has been approved by the Cold QCD/Spin Physics Working Group and the paper god-parent committee, and is undergoing Collaboration review. Once the Collaboration suggestions have been addressed, it will be submitted to Phys. Rev. D.

Forward rapidity jet production provides an alternative approach to obtain constraints on gluon polarization at low  $x$ . Our post-doc, Dr. Ting Lin, performed the first measurement of  $A_{LL}$  for di-jets with at least one of the jets reconstructed within the pseudorapidity range  $0.8 < \eta < 1.8$  for his dissertation. This analysis was complicated by the fact that the tracking efficiency of the STAR Time Projection Chamber falls rapidly when the track pseudorapidity goes beyond  $\eta \sim 1.3$ . Dr. Lin utilized machine learning techniques to overcome this limitation. His results were published last year [1]. As shown in Fig. 1 right panels, the final results are plotted as a function of the di-jet invariant mass for three different di-jet event topologies: di-jets in which one jet is detected in the east half of the Barrel EMC ( $-0.8 < \eta < 0.0$ ) or in the west half of the Barrel EMC ( $0.0 < \eta < 0.8$ ), while the other is in the Endcap EMC ( $0.8 < \eta < 1.8$ ); and events in which both jets fall into the Endcap EMC. The results are also compared to theoretical model predictions from the DSSV and NNPDF groups, which were generated using the DSSV2014 [2] and NNPDFpol1.1 [3] polarized PDF sets. Both of these global analyses include the data from the STAR 2009 inclusive jet analysis [4].

The momentum fractions,  $x_1$  and  $x_2$ , carried by the two interacting partons in the hard scattering, which are probed by these results, are shown in Fig. 1 left panels for the lowest di-jet mass bin. To map with the asymmetry results, the momentum fraction distributions are also separated into the same three event topologies. It is obvious from the distributions that different topologies probe different ranges of the momentum fractions, and as the di-jet goes to higher pseudorapidity,  $x_2$  shifts to lower values and the separation between  $x_1$  and  $x_2$  increases. These results are still limited by the poor statistics especially for both jets going to the higher pseudorapidity region, but with more data from 2012, 2013, and 2015, it will

be an important basis for further analysis at higher pseudorapidity values. Dr. Lin won the 2018 RHIC&AGS Thesis Prize for his dissertation.

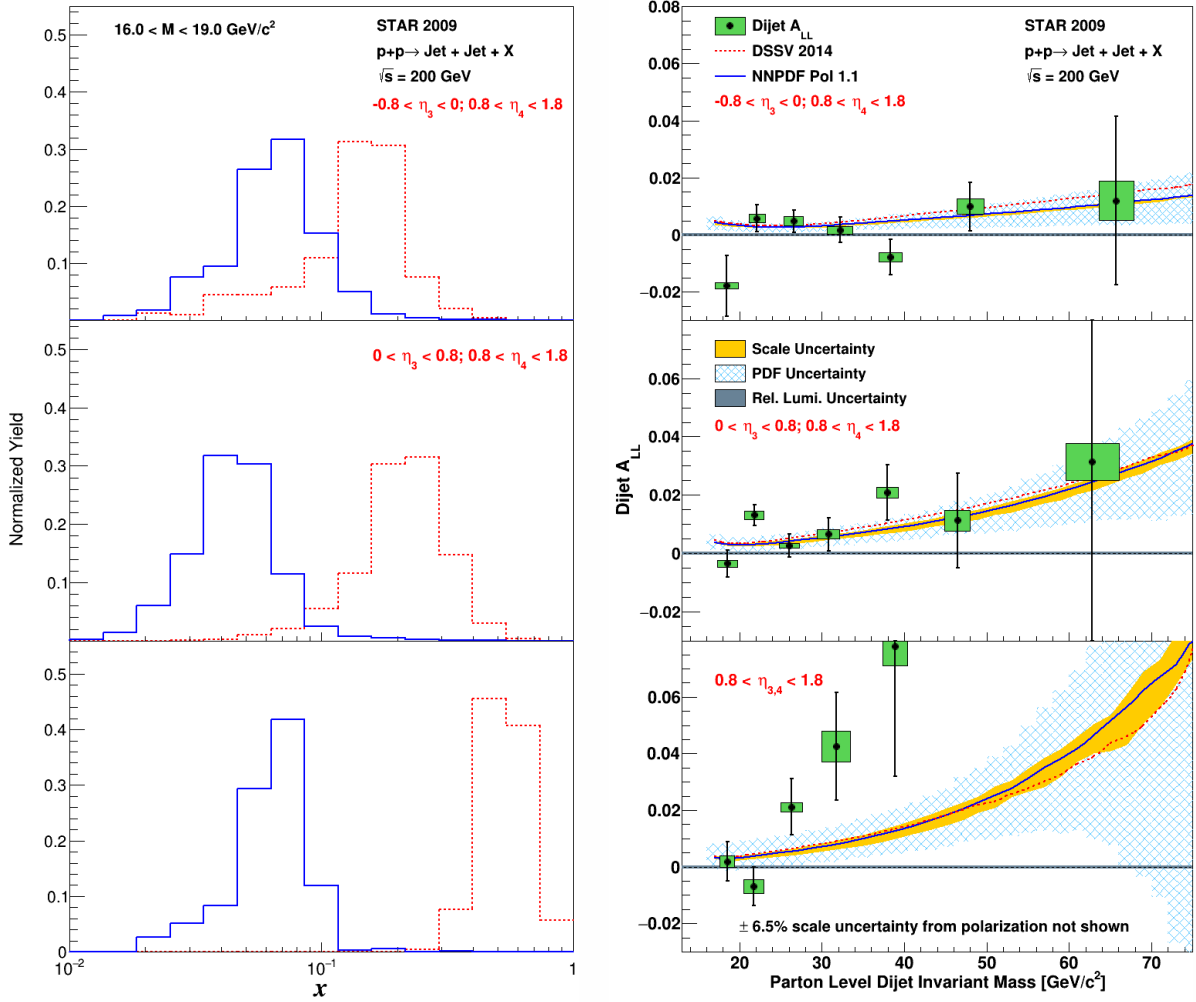


**FIG. 1.** (Left) The distribution of the parton  $x_1$  and  $x_2$  for di-jets with different jet pseudorapidity. (Right)  $A_{LL}$  as function of parton level di-jet invariant mass with different di-jet configurations.

We are also actively investigating transverse spin phenomena at RHIC. Transversity, together with the unpolarized and helicity distributions, are the three leading-twist distributions in the proton. However, much less is known about the transversity distribution because it is chiral odd. The Collins effect convolutes the chiral-odd quark transversity distribution with the chiral-odd Collins fragmentation function, an azimuthal modulation of pion production about the thrust axis of a jet that arises from a transversely polarized quark. It has been observed in semi-inclusive deep-inelastic scattering (SIDIS) by HERMES and COMPASS. The Collins effect is known to be universal in  $e^+e^-$  collisions and SIDIS. It has also been argued [5] that the universality of the Collins effect extends to  $pp$  collisions if the appropriate jet reconstruction algorithm – *e.g.*, the anti- $k_T$  algorithm – is used.

As discussed in last year's *Progress in Research*, in early 2018 we published the first ever observation of the Collins effect in  $pp$  collisions [6], based on an analysis of 500 GeV data that STAR recorded during 2011. Since then, we have focused on completing and publishing a companion article providing the first-ever investigation of the Collins effect in 200 GeV  $pp$  collisions, based on data that STAR recorded during 2012. The 200 GeV data from 2012 probe the Collins effect in the region  $0.1 < x < 0.3$ , which coincides with the peak of the transversity distribution in recent global analyses. When sampling the same  $x$  range, the observed asymmetries in the 2012 data are consistent with those we found in [6]. However, the much greater statistics of the 2012 data set bring additional features into focus. For example, Fig. 2 shows that, when the asymmetry is plotted vs.  $j_T$ , the momentum of the pion transverse to the jet axis, the peak is observed to shift to higher  $j_T$  as the hadron longitudinal momentum fraction within the jet,  $z$ , increases. This feature had not been predicted in previous model calculations of the Collins effect. The draft paper describing the 2012 Collins effect analysis and results is nearly ready for the god-parent committee.

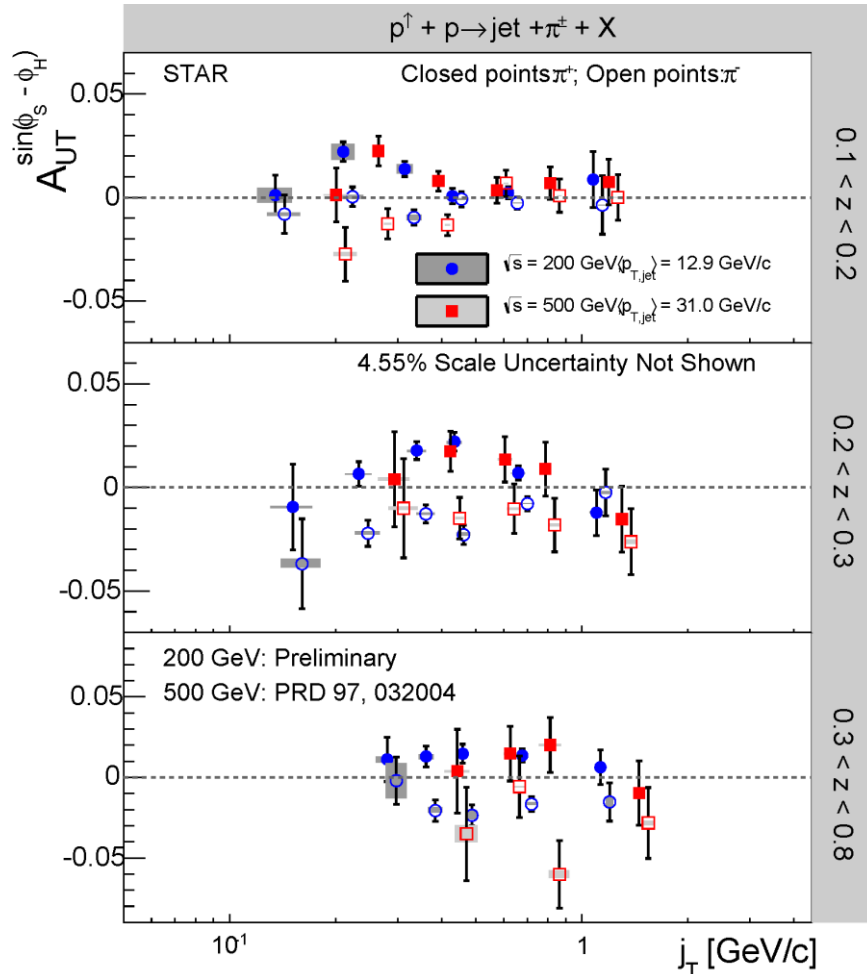


**FIG. 2.** Collins asymmetry vs  $j_T$ , the hadron momentum transverse to the jet thrust axis, for three different ranges of hadron momentum fraction  $z$  within the jet. The 500 GeV results in red are from [6]. The 200 GeV results in blue are preliminary.

We are also performing a similar Collins effect analysis based on the much larger 200 GeV data set that STAR recorded during 2015. The high statistics of the 2015 data set will permit the results to be presented as three-dimensional functions of jet  $p_T$ , hadron  $z$ , and hadron  $j_T$ . This fine-grained presentation will provide powerful new constraints for global analyses of the Collins effect, and might elucidate unexpected features, as we've already seen in Fig. 2. On the other hand, the high statistics of the 2015 data set has required us to develop a number of improved analysis procedures in order to minimize the systematic uncertainties.

The STAR Heavy Flavor Tracker was installed during the 2015 RHIC run, significantly increasing the material budget in the middle of STAR compared to the 2011 500 GeV and 2012 200 GeV data sets. So we need a very good understanding of background contributions and the particle identification (PID). Pure samples of protons and pions for PID studies have been obtained using the reconstructed weak decays of the Lambda, anti-Lambda and the short-lived neutral kaon through the  $\Lambda \rightarrow p + \pi^-$ ,  $\bar{\Lambda} \rightarrow \bar{p} + \pi^+$  and  $K_S \rightarrow \pi^+ + \pi^-$  decay channels. For example, Fig. 3 left panel shows the reconstructed Lambda invariant mass for the momentum range 0.8 - 0.85 GeV/c. A parameter  $n_\sigma(\pi)$ , which relates the measured energy loss  $dE/dx$  (GeV/cm) of the charged particles to the expected value for pions, is used to identify different particles. The  $n_\sigma(\pi)$  of the identified pions and protons as functions of the momentum from this PID study are shown in Fig. 3 right panel.

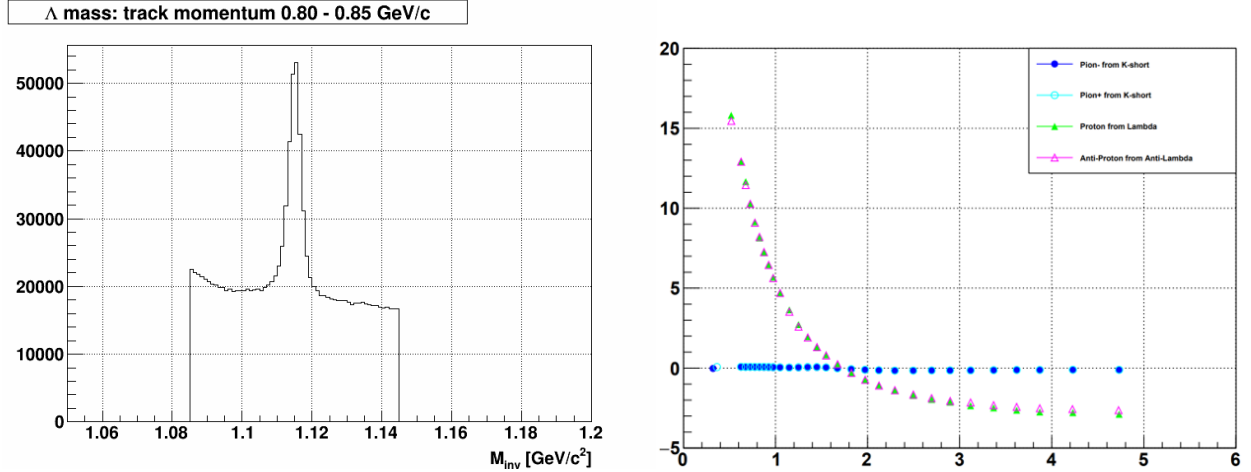


**FIG. 3.** (Left) Reconstructed Lambda mass for the momentum range 0.8 – 0.85 GeV/c. (Right)  $n_\sigma(\pi)$  from the identified pions (from  $K_S$ ) and protons (from  $\Lambda$ ) as functions of the momentum values.

We have also investigated the underlying event contributions to the jets using the off-axis cone method. Generally, the underlying event background is relatively small. However, it can become very large in low- $p_T$  jets at high  $j_T$ . In Fig. 4 left panel, the red curve shows the  $j_T$  distribution of the tracks inside the jets while the blue one shows the estimated underlying event background, combined with the bottom ratio curve (background over the total yield). Figure 4 shows that the nominal underlying event background can be as large, or larger, than the total signal, which points to a problem estimating the background contribution in the jet periphery. Jets are reconstructed using the anti- $k_T$  algorithm, which is

not a precise circular area, while the background from the off-axis cone method is strictly fixed as a cone with the same radius as the jet. We performed several different studies and finally decided to use a  $j_T$  upper limit cut in the analysis in order to minimize the uncertainty in underlying event subtraction. The track  $j_T$  range varies with hadron  $z$  and jet  $p_T$ , so we chose to make the upper  $j_T$  limit  $p_T$  and  $z$  dependent. After some cut optimizations,  $j_T < (0.025 + 0.3295 \times z) \times p_T$ , was selected. The right panel in Fig. 4 shows the same plots as the left panel but after the implementation of this upper  $j_T$  cut. A significant fraction of the background is removed, while this cut has very little impact on the signal yields. We also performed similar studies for a range of jet radii and with the mid-point cone and  $k_T$  jet reconstruction algorithms that sample the jet periphery differently from anti- $k_T$ . We have found that the difference between the anti- $k_T$  and  $k_T$  algorithm background fractions can be used to estimate the systematic uncertainty for this method.

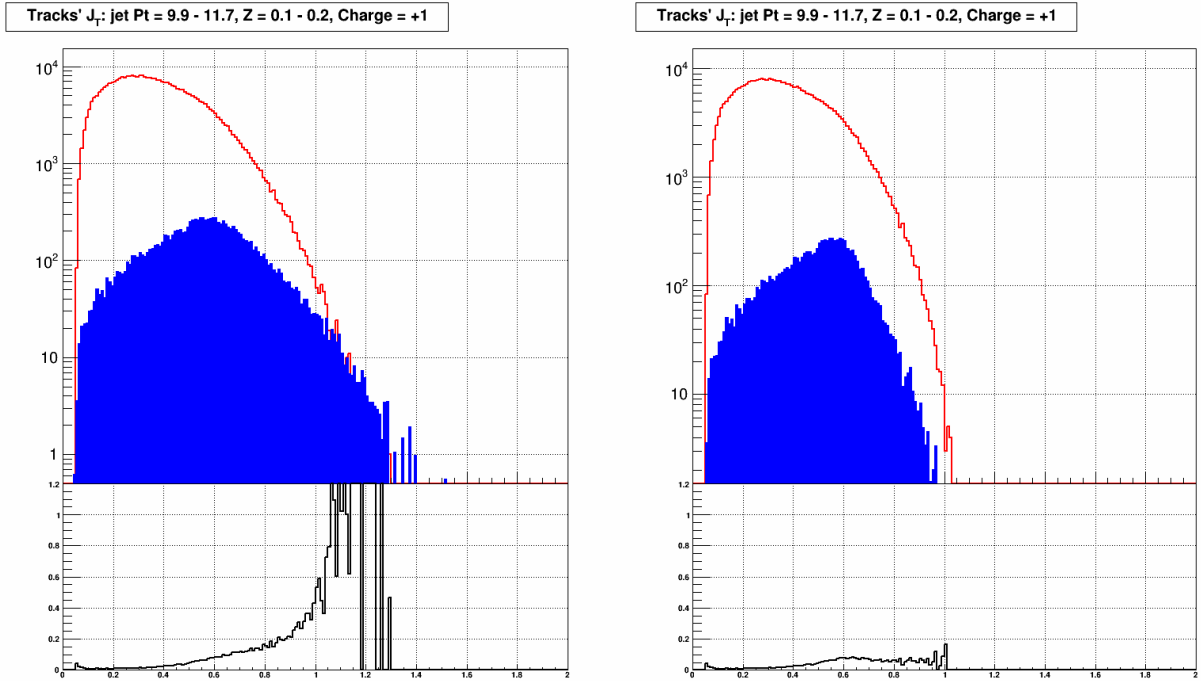


**FIG. 4.** (Left) The track  $j_T$  distributions before the  $j_T$  upper limit cut for tracks inside the jets (red curve) and from the off-axis cone method (blue curve). (Right) The track  $j_T$  distributions after the  $j_T$  upper limit cut for tracks inside the jets (red curve) and from the off-axis cone method (blue curve). The bottom panels are the ratio of the background over the total yield.

Finally, we continue to carry various administrative responsibilities for STAR. Dr. Gagliardi is one of the two conveners of the Cold QCD and Spin Physics Working Group. Dr. Lin is serving as the software coordinator for the EEMC. Dr. Gagliardi served on the god-parent committee for four papers [1,7-9] during the past year. Dr. Lin also served on the god-parent committee for three of them [1,7,8].

[1] J. Adam *et al.* (STAR Collaboration), Phys. Rev. D **98**, 032011 (2018).

[2] D. de Florian, R. Sassot, M. Stratmann, and W. Vogelsang, Phys. Rev. Lett. **113**, 012001 (2014).

[3] E. R. Nocera *et al.* (NNPDF Collaboration), Nucl. Phys. B **887**, 276 (2014).

- [4] L. Adamczyk *et al.* (STAR Collaboration), Phys. Rev. Lett **115**, 092002 (2015).
- [5] Z.-B. Kang, X. Liu, F. Ringer, and H. Xing, JHEP **11** (2017) 068.
- [6] L. Adamczyk *et al.* (STAR Collaboration), Phys. Rev. D **97**, 032004 (2018).
- [7] J. Adam *et al.* (STAR Collaboration), Phys. Rev. D **98**, 091103(R) (2018).
- [8] J. Adam *et al.* (STAR Collaboration), Phys. Rev. D **98**, 112009 (2018).
- [9] J. Adam *et al.* (STAR Collaboration), Phys. Rev. D **99**, 051102(R) (2019).